Influence of Multivalent Electrolytes on Interionic Correlations: A Grand Canonical Monte Carlo Study of the Electrostatic Stability of Charged Interfaces

A. Delville*

CRMD, CNRS, 1B rue de la Férollerie, 45071 Orléans Cedex 02, France

Received: March 1, 2002; In Final Form: May 31, 2002

We use grand canonical Monte Carlo simulations in the framework of the primitive model to determine the mechanical stability of planar charged interfaces in the presence of various salts of multivalent counterions. Our intent is to determine the influence of salt addition on the strength and the range of interionic correlations. Despite the simplicity of the primitive model, the equation of state of these interfacial systems exhibits complex behavior because the addition of salts of di- and trivalent counterions enhances the interionic correlations and induces the coexistence of two phases composed of differently swollen interfaces. The occurrence of such phase coexistence is related to the inversion of the apparent interfacial charge and the accumulation of salt in the interfacial domain by contrast with the Donnan exclusion phenomenon.

I. Introduction

Monitoring the long-range electrostatic stability of charged interfaces is an important consideration for the optimization of a large variety of natural (membrane fusion, DNA condensation, etc.) and industrial (soil and colloidal science) processes in which they play central roles. Many years ago,[1−3] the importance of the overlap between the diffuse layers of monovalent counterions surrounding the charged particles was clearly identified as the source of their so-called "electrostatic repulsion". More recent numerical treatments[4−7] were necessary to identify and quantify the role of the interionic correlations on the mechanical behavior of the charged interfaces neutralized by di- or trivalent counterions. In the framework of the primitive model,[8] the net stability of these charged interfaces was shown to result from a delicate balance between antagonistic contributions.[7] If interionic correlations are negligible, the mechanical behavior of charged colloids is driven by the entropic repulsion resulting from the overlap of the diffuse layer of counterions surrounding each particle. That contribution may be evaluated from the counterions' average concentration halfway between the colloids. Interionic correlations were shown to be negligible under the condition of weak electrostatic coupling[7,9] (i.e., for a coupling parameter ξ smaller than 0.05 [$\xi = (ez_i d\sigma)/(4\pi\epsilon_0\epsilon_r kT)$, where σ is the surface charge density of the interface and d is the minimum counterion/surface separation]). Otherwise, interionic correlations become important and introduce two other contributions to the net interfacial interaction:[7,9] an electrostatic attraction and a repulsion resulting from the contact forces between the counterions. This contact contribution becomes the driving source of repulsion[7] when the ionic size increases too much. As a consequence, the net behavior of these materials is difficult to predict without accurate numerical simulations that are able to describe and quantify these phenomena without any approximations or systematic errors.

Despite the numerous studies devoted to this problem,[4−7,9−14] some questions , such as the influence of salt addition on these interionic correlations and thus the stability of the charged interfaces, have not been completely answered. In the presence of salt, one generally expects a large decrease of the attractive forces induced by the interionic correlations because of the corresponding screening[15,16] of the interfacial correlation length. By contrast, in the presence of monovalent counterions, one notes a strong attenuation of the entropic repulsion resulting from the Donnan exclusion phenomenon.[17] Therefore, no simple guideline emerges that could be used to predict qualitatively the behavior of charged colloids in the presence of salts of various valence. Another question concerns the salt-exclusion phenomenon: Is it a general phenomenon that occurs also for salts of multivalent counterions? Finally, no one seems to have considered the contribution of the contact forces that becomes overwhelming when the salt volume fraction increases in the interfacial domain.

Recently, a new theory of ionic condensation was introduced for the interpretation of the re-entrant condensation of polyions[18−23] in the presence of increasing concentration of salts of multivalent counterions. One interesting feature of this semiempirical treatment is the identification of the inversion of the apparent charge[21−23] of the surfaces as the key phenomenon responsible for the resolubilization of aggregated polyions.

We used Monte Carlo simulations in the grand canonical ensemble[24] to answer these questions by determining the number of salt molecules confined between two parallel charged plates as a function of their separation, of the salt concentration, and of the valence of both the counter- and co-ions. For each system, we determined the net force exerted between the charged surfaces and tried to establish a relationship between the occurrence of the inversion of the apparent charge of the interfaces and a possible coexistence between collapsed and stabilized interfaces.

II. Methods

The grand canonical Monte Carlo (GCMC)[24] simulations were performed at 298 K in the framework of the primitive model by using the dielectric constant of bulk water. The simulation cell results from the stacking of five charged interfaces constituted from a liquid-phase confined between two structureless infinite lamellae with a thickness of 10 Å to mimic

* E-mail: delville@cnrs-orleans.fr.

10.1021/jp020600f CCC: $22.00
Published on Web 07/18/2002

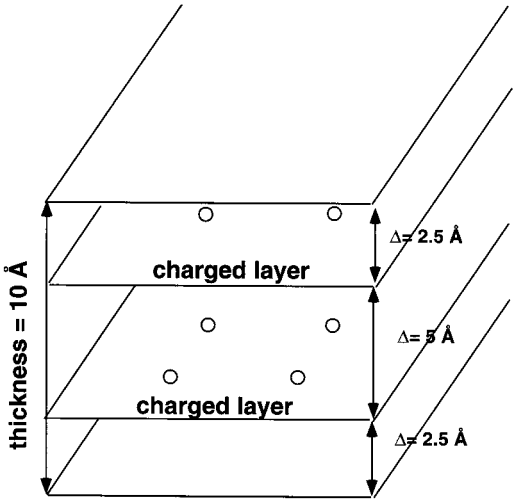

Figure 1. Illustration of the two networks of charged sites distributed within each lamella.

clay particles. The period of one elementary interface is the same within the whole stack and varies between 16 and 85 Å. The ionic radius was set equal to 2.5 Å to mimic the hydration shells[25] of sodium and calcium cations. As shown in Figure 1, two squared networks of monovalent sites are distributed within each of the lamellae and are located 2.5 Å from their basal surfaces. The grand canonical Monte Carlo simulations were performed for mono-, di-, and trivalent counterions in the presence of 1:1 or 2:1 and 2:2 or 3:1 and 3:3 salts, respectively.

In the general case of a z_1/z_2 electrolyte in bulk solution, the ionic concentration (c_i) is related to the salt concentration (c_{salt}) by the relationship $c_i = \nu_i c_{salt}$ with $z_1\nu_1 + z_2\nu_2 = 0$ for electroneutrality. The ionic strength is defined by

$$I = \frac{1}{2} c_{salt}(\nu_1 z_1^2 + \nu_2 z_2^2) \tag{1}$$

The partition function of the grand canonical ensemble for these bulk electrolyte solutions is given by

$$\Xi(\gamma_\pm, V, T) = \sum_{N_1} \left(\frac{V}{\lambda_1^3}\right)^{N_1} \frac{\exp(\beta N_1 \mu_1)}{N_1!} \sum_{N_2;\, z_1 N_1 + z_2 N_2 = 0} \left(\frac{V}{\lambda_2^3}\right)^{N_2} \frac{\exp(\beta N_2 \mu_2)}{N_2!} \int \ldots \int \exp(-\beta E)\, d\vec{\tau}_1 \ldots d\vec{\tau}_N \tag{2}$$

where the ionic chemical potential (μ_i) satisfies the relationship

$$B_i = \beta\mu_i + \ln\left(\frac{V}{\lambda_i^3}\right) = \ln(c_{salt}\nu_i\gamma_i V) \tag{3}$$

in which the ionic activity coefficient (γ_i) is related to the salt activity coefficient ($\gamma_\pm$) by

$$\gamma_\pm^{(\nu_1+\nu_2)} = \gamma_1^{\nu_1}\gamma_2^{\nu_2} \tag{4}$$

Using eqs 3 and 4, eq 2 simplifies to

$$\Xi(\gamma_\pm, V, T) = \sum_{N_1} \sum_{N_2;\, z_1 N_1 + z_2 N_2 = 0} \frac{\exp(N_1 B_1 + N_2 B_2)}{N_1! N_2!} \int \ldots \int \exp(-\beta E)\, d\vec{\tau}_1 \ldots d\vec{\tau}_N \tag{5}$$

Monte Carlo sampling of this grand canonical ensemble is performed by selecting, with equal probability, either randomly moving one ion, adding a dissociated salt molecule, or simultaneously removing ν_1 cations and ν_2 anions corresponding to a salt molecule. To satisfy the detailed balance condition,[26] the probability of adding one salt molecule, or in other words switching from the (N_1, N_2) system to the ($N_1 + \nu_1$, $N_2 + \nu_2$) system, is directly derived from eq 5:

$$P_{add} = \min\left(1, \frac{\exp(\nu_1 B_1 + \nu_2 B_2)\exp(-\beta\Delta E)}{(N_1+1)\ldots(N_1+\nu_1)(N_2+1)\ldots(N_2+\nu_2)}\right) \tag{6}$$

In the same manner, the probability of removing one salt molecule (i.e., switching from the (N_1, N_2) system to the ($N_1 - \nu_1$, $N_2 - \nu_2$) system) is given by

$$P_{rem} = \min\left(1, \frac{N_1\ldots(N_1-\nu_1+1)\, N_2\ldots(N_2-\nu_2+1)\exp(-\beta\Delta E)}{\exp(\nu_1 B_1 + \nu_2 B_2)}\right) \tag{7}$$

For interfacial systems, eqs 2−7 are still valid, except for the electroneutrality condition that becomes $N_1 z_1 + N_2 z_2 + N_s z_s = 0$, where N_s stems from the total number of charged sites within one interface and z_s, their valence. In other words, it is not possible to distinguish the counterions neutralizing the surface sites from those arising from the salt addition. For each interfacial system, the GCMC simulations are performed with reservoirs at three different ionic strengths (10^{-3}, 10^{-1}, and 1 M) corresponding to Debye screening lengths[27] of 100, 10, and 3 Å, respectively. The chemical potential of the pure salt solutions is determined by preliminary grand canonical Monte Carlo simulations of the bulk solutions. The osmotic pressure of the same salt solutions is derived from a calculation of the virial[28] coefficient performed during Monte Carlo simulations in the canonical ensemble. The electrostatic energy and the electrostatic contribution to the net force acting between any pair of ions in these homogeneous salt solutions are calculated by using classical 3D Ewald summation.[29]

The results are fitted by the following simple analytical laws

$$\gamma_\pm = \exp\left(\frac{-a\sqrt{I}}{1+b\sqrt{I}}\right) + cI + dI^{1.5} + eI^2 \tag{8a}$$

$$\Pi = kT(f\sqrt{I} + gI + hI^2 + mI^3) \tag{8b}$$

that extend the range of validity of the classical Debye−Hückel approximation to ionic strength greater than 1 M.

In all interfacial systems considered here, the surface charge density of the lamellae is set equal to 10^{-2} e/Å^2 to describe a large variety of charged colloids (clays,[30] silica,[31] metallic oxides,[31] etc.). The simulations were performed for lamellae bearing either 200 elementary monovalent charges, in the case of the mono- and divalent counterions, or 324 elementary charges, in the case of the trivalent counterions. Simulations were performed with four times more charged sites to check for the convergence of the Monte Carlo procedure. The electrostatic energy of the stack of five interfaces was evaluated by using the 3D Ewald summation with 3D periodic boundary conditions and the minimum image convention.[32] The total electrostatic energy is given by[29]

$$E_{\text{elect}} = E_{\text{dir}} + E_{\text{rec}} + E_{\text{mom}} + E_{\text{self}} \quad (9a)$$

$$E_{\text{dir}} = \frac{1}{8\pi\epsilon_0\epsilon_r}\sum_{i=1}^{N_i} q_i \sum_{j=1,i\neq j}^{N_j} \frac{q_j \operatorname{erfc}(\kappa r_{ij})}{r_{ij}} \quad (9b)$$

$$E_{\text{rec}} = \frac{1}{2V\epsilon_0\epsilon_r}\sum_{\vec{K},|K|\neq 0} \frac{\exp(-|\vec{K}|^2/4\kappa^2)}{|\vec{K}|^2} \left[\left\{\sum_i q_i \cos(\vec{K}\times\vec{r}_i)\right\}^2 + \left\{\sum_j q_j \sin(\vec{K}\times\vec{r}_j)\right\}^2\right] \quad (9c)$$

$$E_{\text{mom}} = \frac{1}{2V(1+2\epsilon_\infty)\epsilon_0\epsilon_r}\left(\sum_{i=1} q_i \vec{r}_i\right)^2 \quad (9d)$$

$$E_{\text{self}} = \frac{-\kappa}{4\pi^{3/2}\epsilon_0\epsilon_r}\sum_i q_i^2 \quad (9e)$$

The screening parameter κ is set equal to 0.07 Å^{-1}, and 2196 replicas are used for the summation in the reciprocal space, allowing for the use of a spherical cutoff of the electrostatic energy with a relative accuracy[33] better than 10^{-3}. The simulation cell and its replica are immersed in a conducting medium ($\epsilon_\infty = \infty$).

As done previously, the pressure inside each interface is evaluated by using a fictitious reference plane[6−7,10] parallel to the charged surfaces that divides the interface in two subdomains. The total pressure is evaluated by summing the longitudinal components of the electrostatic and contact forces transmitted between these two subdomains across the reference plane, in addition to the entropic contribution resulting from the ionic densities at the reference plane. To increase the accuracy of this numerical method, the reference plate is located halfway between the charged surfaces because, at equilibrium, the longitudinal component of the pressure tensor is uniform within the whole interface. The osmotic pressure (Π) of the interface is evaluated by removing the osmotic pressure of the salt reservoir from the longitudinal component of the pressure tensor averaged within the five charged interfaces. The numerical data and their standard deviations are calculated by using block averages, with the size of the block equal to at least 10 times the total number of ions located within the stack of charged interfaces and at least 1000 blocks for the thermalization step; this calculation is carried out twice for the production step of the Monte Carlo procedure.

III. Results and Discussion

A. Monovalent Counterions. Figure 2 displays the equation of state of charged lamellae neutralized by monovalent counterions in the presence of a 1:1 salt. In all cases, the charged interfaces repel each other because no van der Waals dispersion forces are included in this model. At interlamellar separations smaller than the Debye screening length determined from the salt concentration in the reservoir, the swelling pressure decreases according to a power law and matches the pressure calculated for salt-free interfaces. At larger separations, the swelling pressure decreases according to an exponential law, with an exponent fixed by the same Debye length. Simultaneously, the salt concentration within the interface is smaller than its value in the reservoir (Figure 3) when the interlamellar separation is smaller than the Debye length. This Donnan exclusion phenomenon is well described in the framework of the Poisson−Boltzmann formalism,[17] and it is responsible for the exponential decrease of the swelling pressure[17] of the interfaces in equilibrium with a salt reservoir.

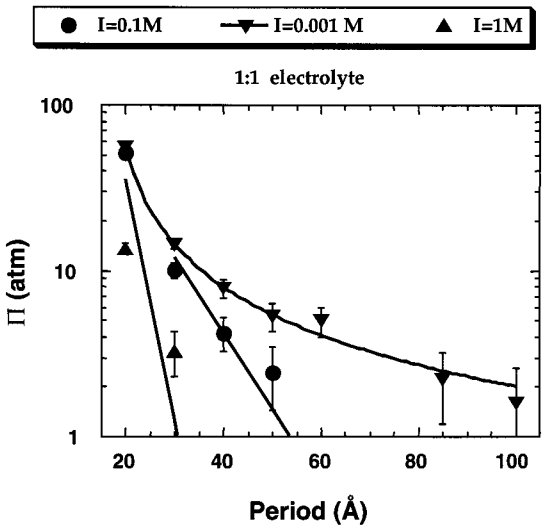

Figure 2. Swelling pressure of the charged interfaces in the presence of a 1:1 electrolyte.

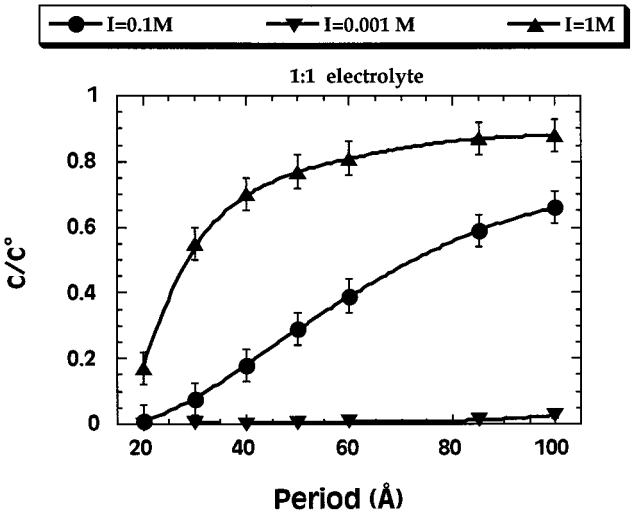

Figure 3. Exclusion of the 1:1 electrolyte from the charged interfaces.

Typical counterion and co-ion concentration profiles are displayed in Figure 4 in addition to the residual apparent charge of the surface resulting from the integration of the local ionic densities:

$$q_{\text{app}}(z) = q_{\text{surf}} - \frac{e}{s}\int_0^z (z_+c_+(z) + z_-c_-(z))\,dz \quad (10)$$

where e is the electronic charge and s the lateral section of the simulation cell. The data shown in Figure 4a and b correspond to charged interfaces in equilibrium with salt reservoirs of ionic strengths 10^{-1} and 1 M, respectively. At low ionic strengths and for small interlamellar separations (the period is 50 Å in Figure 4a), the two ionic concentration profiles do not overlap, and the apparent charge increases monotonically from the nominal charge of the surface (q_{surf}) to zero halfway between the lamellae because of the average electroneutrality of each half-cell. But at greater ionic strengths (Figure 4b) or interlamellar separations (not shown), the counterion and co-ion concentration profiles overlap significantly, and the apparent charge exhibits oscillations with an inversion of sign. To detect systematically the occurrence of this charge inversion and to quantify its intensity, let us define the maximum value of the overcharging fraction (see Figure 5) by the largest value of the

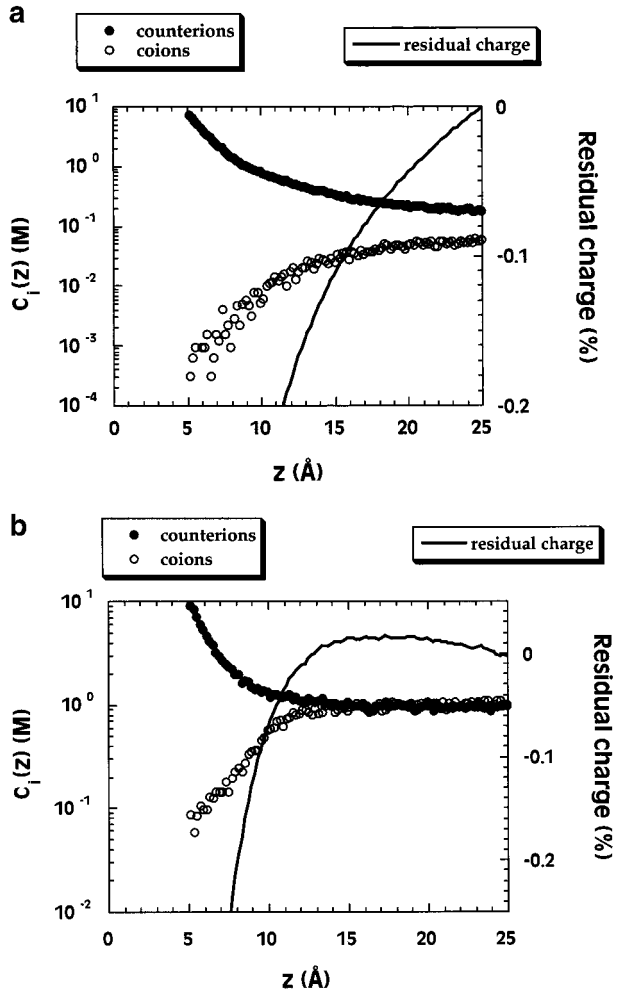

Figure 4. Local ionic concentration profiles and residual charge within the interfaces (see text) for a 1:1 electrolyte at $I = 0.1$ M (a) and $I = 1$ M (b).

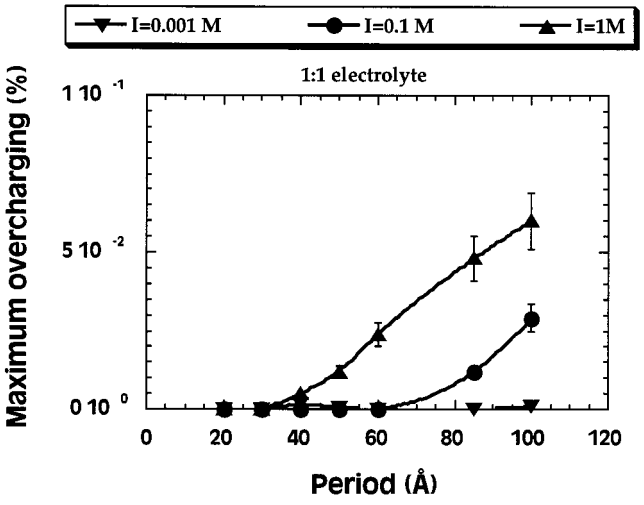

Figure 5. Maximum overcharging of the interfaces in the presence of a 1:1 electrolyte.

ratio $-q_{app}(z)/q_{surf}$ evaluated over the whole interlamellar space:

$$\text{maximum}_{z\in[0,P/2]}\left(-\frac{q_{app}(z)}{q_{surf}}\right) \qquad (11)$$

As shown in Figure 4a, this maximum is equal to zero when the ionic concentration profiles do not overlap. The plot of

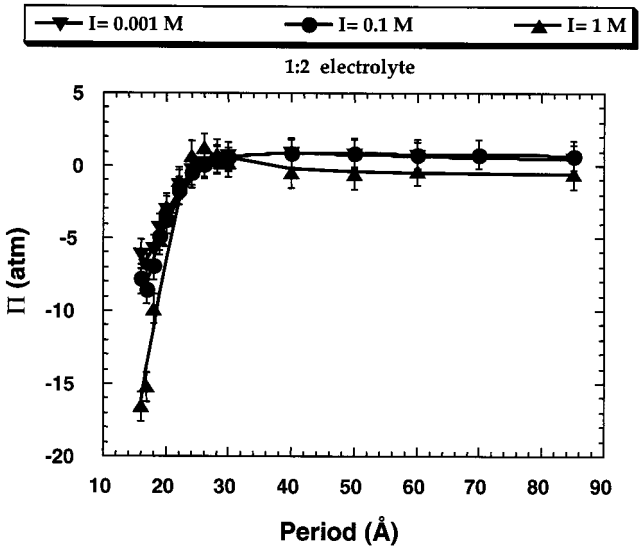

Figure 6. Equation of state of the charged interfaces in the presence of a 1:2 salt.

Figure 5 confirms the general trend discussed above: an increase of the interlamellar separation or the salt concentration of the reservoir increases the occurrence of this overcharging phenomenon that is not specific to multivalent counterions.

B. Divalent Counterions. The net force exerted between lamellae neutralized by divalent counterions in the presence of a small amount of a 2:1 electrolyte (10^{-3} M $\leq I \leq 10^{-1}$ M, see Figure 6) is equivalent to the force previously calculated without salt.[6−7,10] At small separations ($P < 20$ Å), a strong attraction is detected because of noticeable interionic correlations whereas the ion−ion repulsion remains negligible. By contrast, above 30 Å, no significant force is detected because these antagonistic attractive/repulsive contributions cancel each other. Furthermore, adding salt to this interfacial system does not screen the correlation forces but rather enhances the strength of the electrostatic attraction detected at small separations ($P < 20$ Å). At high ionic strength ($I = 1$ M), an intriguing crossover is detected at $P \approx 25$ Å where a reduced repulsion ($\Pi = 1$ atm) emerges from the statistical noise. As a consequence, if the external constraint is lower than this limiting value, these charged interfaces may coexist at two different interlamellar separations. Such mechanical behavior has already been detected experimentally[34] and has been suggested to be related to some inversion of the apparent charge of the interface.[34] In agreement with the interpretation previously given,[34] the occurrence of a net repulsion at $P \approx 25$ Å (cf. Figure 6) and the resulting coexistence of swollen ($P > 40$ Å) and collapsed ($P \approx 16$ Å) interfaces correspond to a sharp increase of the overcharging fraction (cf. Figure 7). However, at larger separations ($P > 40$ Å), the overcharging fraction remains constant whereas the swelling pressure decreases to negative values. As a consequence, one may infer that the overcharging phenomenon is necessary but not sufficient to induce the redispersion of coagulated colloids by the addition of a 2:1 salt. Finally, Figure 8 displays the same salt-exclusion phenomenon as that reported for lamellae neutralized by monovalent counterions in the presence of a 1:1 electrolyte.

In the presence of a 2:2 electrolyte (Figures 9−11), the charged interfaces neutralized by divalent counterions display qualitatively the same behaviors that they do in the presence of a 2:1 electrolyte. Replacing the monovalent ions by divalent co-ions slightly shifts the swelling pressure to positive values at large separations ($P > 30$ Å) and weak ionic strengths (10^{-3}

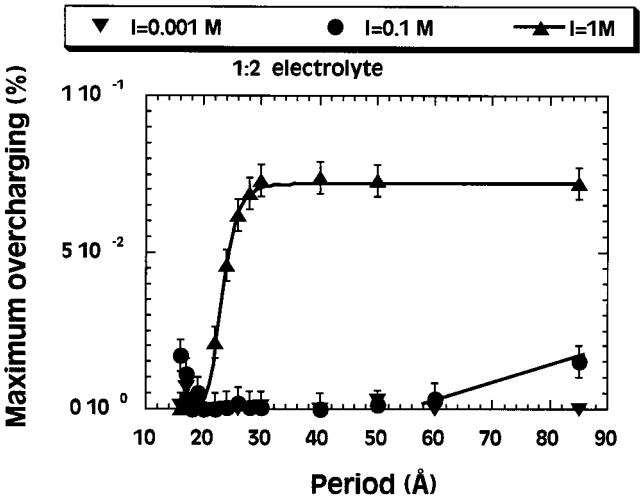

Figure 7. Maximum overcharging detected in the presence of a 1:2 electrolyte.

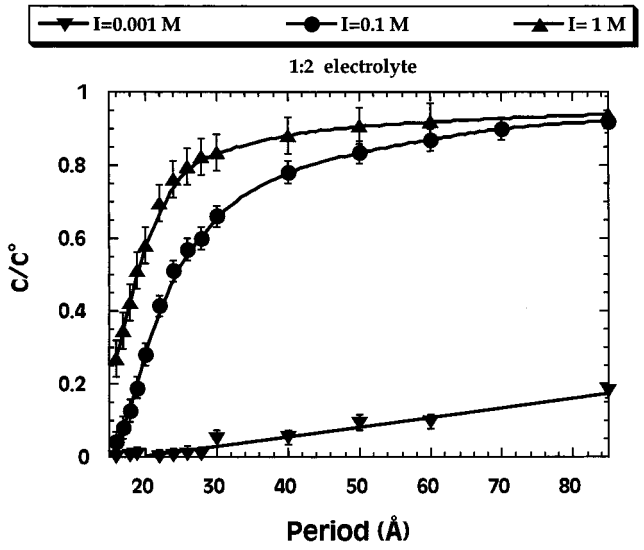

Figure 8. Exclusion of the 1:2 electrolyte from the charged interfaces.

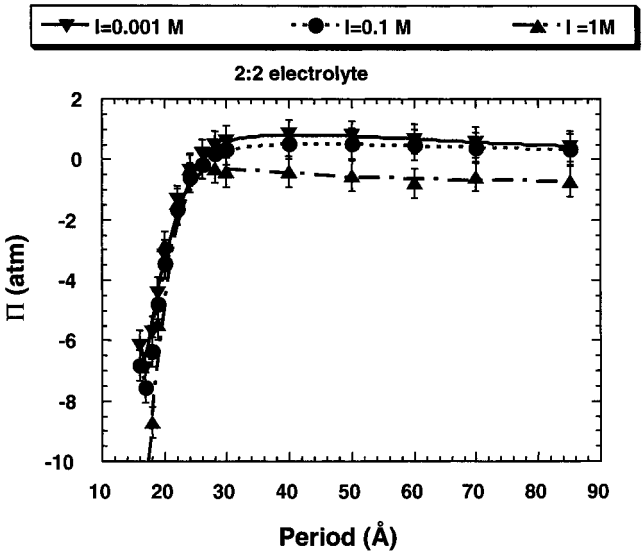

Figure 9. Equation of state of the charged interfaces in the presence of a 2:2 salt.

M $\leq I \leq 10^{-1}$ M, see Figures 6 and 9) whereas a larger amount of salt ($I = 1$ M) reduces the pressure to negative values over the whole range of separations studied here. Nevertheless, a

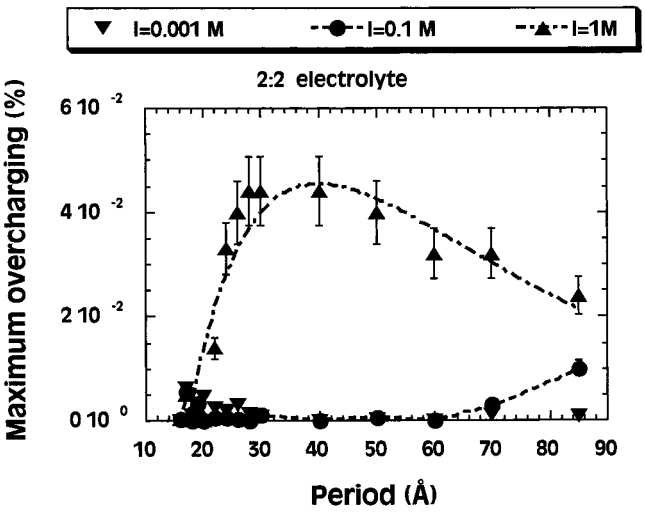

Figure 10. Maximum overcharging of the interfaces in the presence of a 2:2 salt.

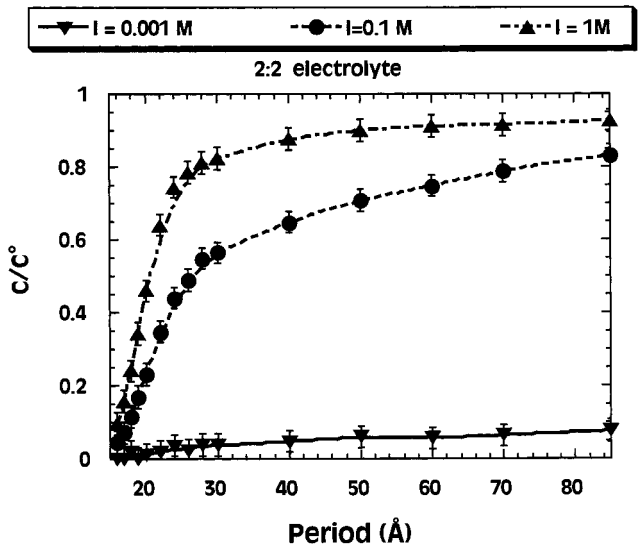

Figure 11. Exclusion of the 2:2 electrolyte from the charged interfaces.

small singularity of the pressure remains detectable at this high ionic strength for $P \approx 25$ Å. Here again, this singularity corresponds to a sudden enhancement of the overcharging ratio (Figure 10), even if the swelling pressure cannot induce redispersion of coagulated interfaces. Finally, Figure 11 exhibits a similar exclusion phenomenon as before (see Figures 3 and 8).

C. Trivalent Counterions. The behavior of charged interfaces neutralized by trivalent counterions in the presence of a 3:1 electrolyte is presented in Figures 12−14. The swelling pressure obtained in the presence of these trivalent counterions (Figure 12) is qualitatively equivalent to that calculated for divalent counterions (Figure 6). Here also, the net force exerted between the interfaces is mainly attractive, and the addition of a large amount of salt ($I = 1$ M) induces a strong singularity at $P \approx 25$ Å, allowing for the coexistence of swollen ($P > 40$ Å) and coagulated ($P \approx 16$ Å) interfaces. The major difference in the mechanical behavior of interfaces neutralized by divalent counterions is the deeper attraction detected at small separations ($P < 20$ Å). The singularity of the swelling pressure detected at the highest salt concentration coincides with a sudden increase in the overcharging phenomenon (see Figures 13 and 7), but now the overcharging phenomenon disappears at larger interlamellar separations ($P > 40$ Å). The major difference between

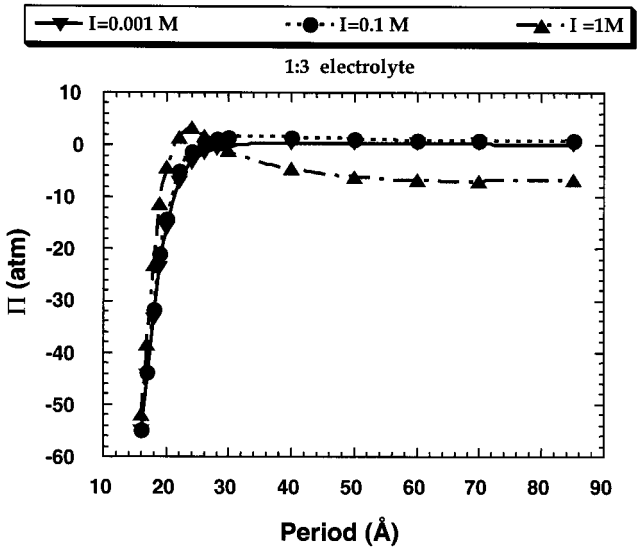

Figure 12. Equation of state of the charged interfaces in the presence of a 1:3 salt.

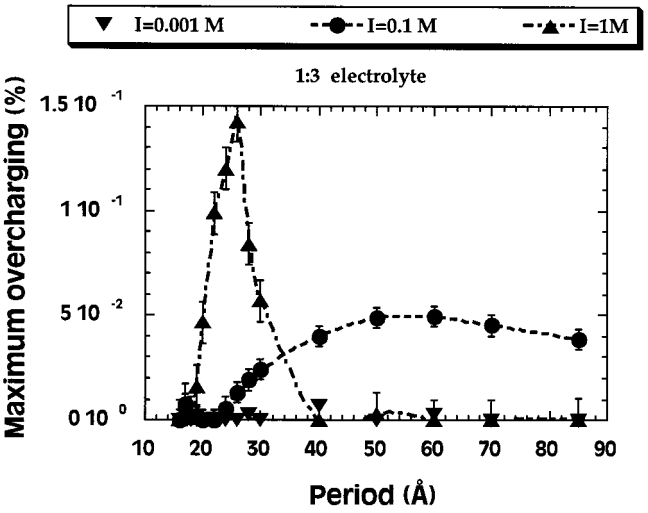

Figure 13. Maximum overcharging of the interfaces in the presence of a 1:3 salt.

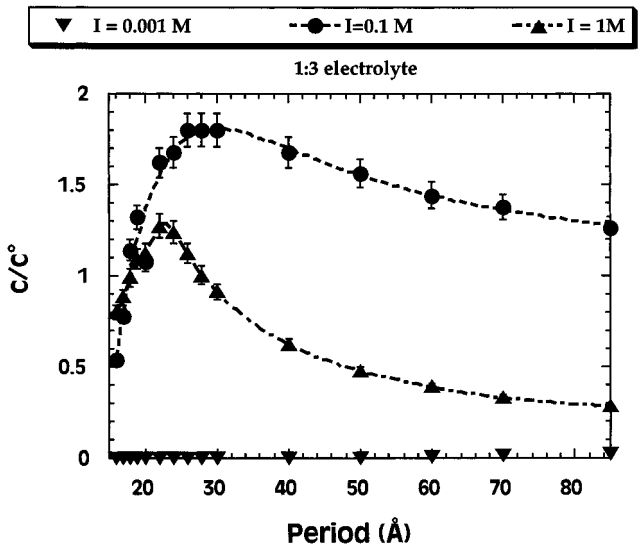

Figure 14. Accumulation of the 1:3 electrolyte within the charged interfaces.

these two interfacial systems is detected from the amount of salt confined within the interlamellar space. Whereas salts of

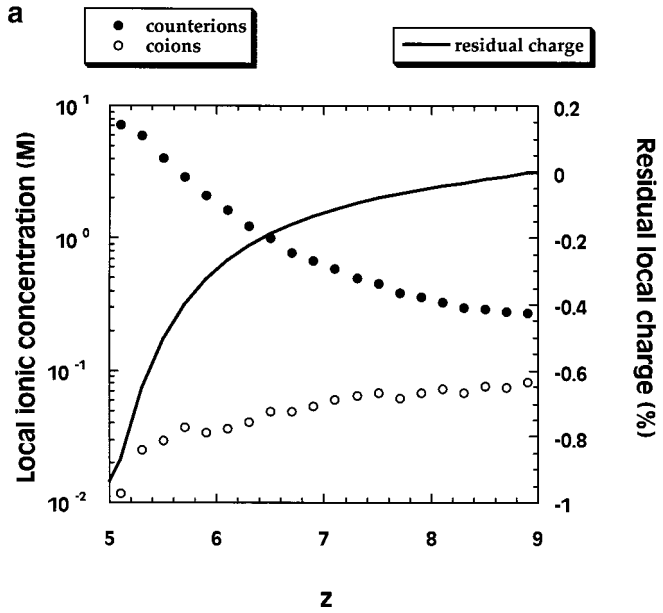

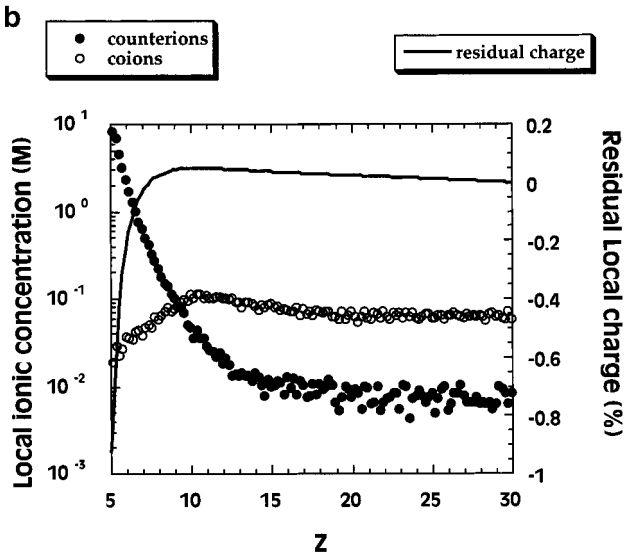

Figure 15. Local ionic concentration profiles and residual charge within the interfaces in the presence of a 1:3 electrolyte at an ionic strength of 0.1 M for $P = 18$ Å (a) and $P = 60$ Å (b).

mono- and divalent counterions are generally depleted (see Figures 3 and 8) by the so-called Donnan exclusion phenomenon, a 3:1 salt is trapped in large excess in the interfacial domain (Figure 14), suggesting the occurrence of strong interionic correlations. The largest excess of salt corresponds to an intermediate ionic strength ($I = 0.1$ M) whereas the maximum of this salt accumulation is detected at reduced interlamellar separations (20 Å $< P <$ 30 Å) corresponding to the minimum separations required to detect noticeable overcharging (cf. Figure 13) and singularity of the swelling pressure (cf. Figure 12). This accumulation of multivalent salts has been reported from Monte Carlo simulations[35] but without establishing any connection with the mechanical stability of these charged interfaces.

The comparison of the average counterion and co-ion concentration profiles calculated at $I = 0.1$ M (Figure 15a and b) better illustrates the connection between this overcharging phenomenon and the interionic correlations. At small interlamellar separations (e.g., $P = 18$ Å in Figure 15a), the ionic concentration profiles are monotonic, and no overcharging occurs. But at $P = 60$ Å (Figure 15b), noticeable overcharging is detected, and the co-ion concentration profile exhibits a

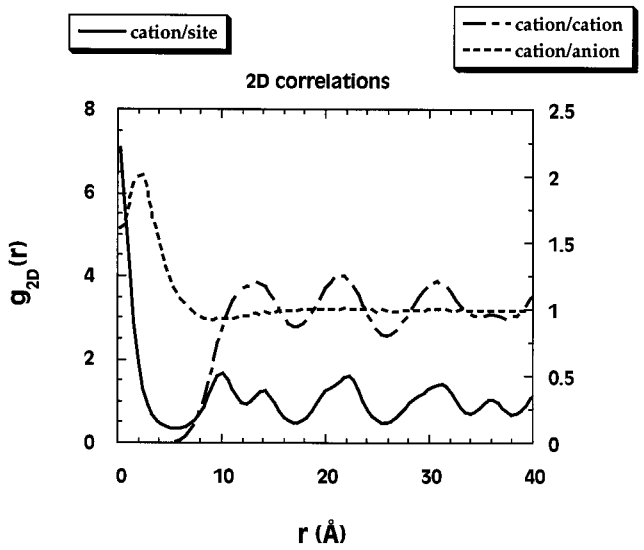

Figure 16. 2D radial distribution functions analyzing the counterion/site, counterion/counterion, and counterion/co-ion structures within the charged interface ($P = 60$ Å) in the presence of a 1:3 electrolyte ($I =$ 0.1 M).

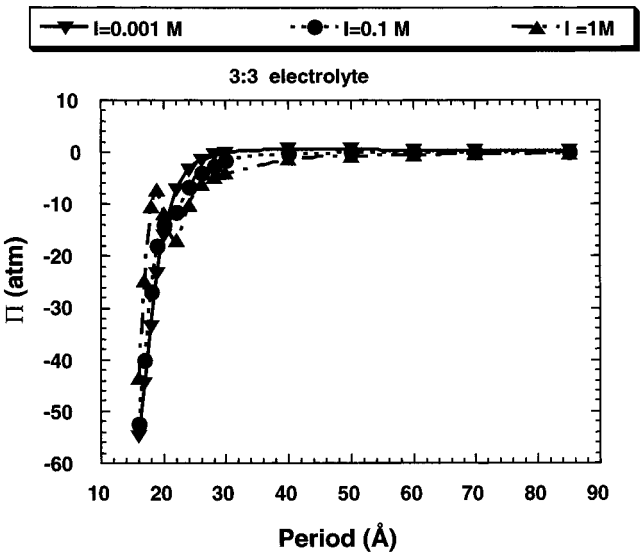

Figure 17. Equation of state of the charged interfaces in the presence of a 3:3 salt.

maximum, suggesting the existence of some counterion/co-ions correlations because both the cation and anion concentration maxima are separated by just one ionic diameter. To further quantify these interionic correlations, we have calculated the 2D radial distribution functions (Figure 16) (1) between the surface sites and the condensed counterions in contact with the solid surface, (2) between the counterions located within the same layer of condensed cations, and (3) between the counterions and the co-ions located within neighboring layers, each corresponding to the maximum of its concentration profile (see Figure 15b).

Because of the strong electrostatic coupling between the surface sites and the trivalent cation, the cation/surface site 2D radial distribution function exhibits a strong ordering that propagates to large distances (>40 Å). This initial ordering is further translated into a large organization of the cation/cation 2D radial distribution function for the cations located within the same condensation layer. Finally, Figure 16 also displays local ion/cation ordering that is the fingerprint of the correlation inferred from Figure 15b.

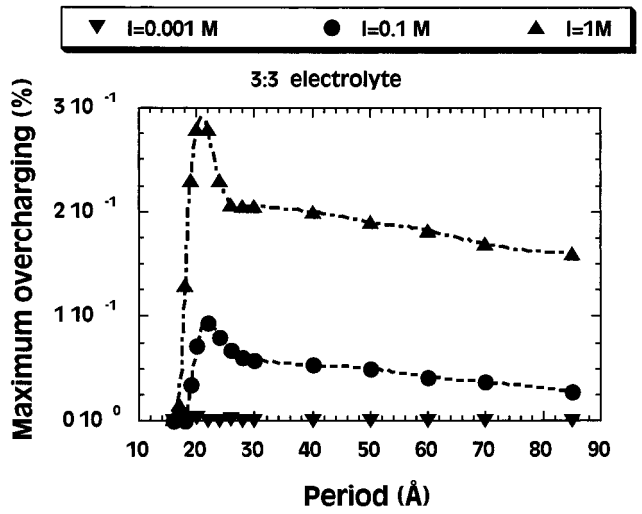

Figure 18. Ratio of maximum overcharging detected in the presence of a 3:3 salt.

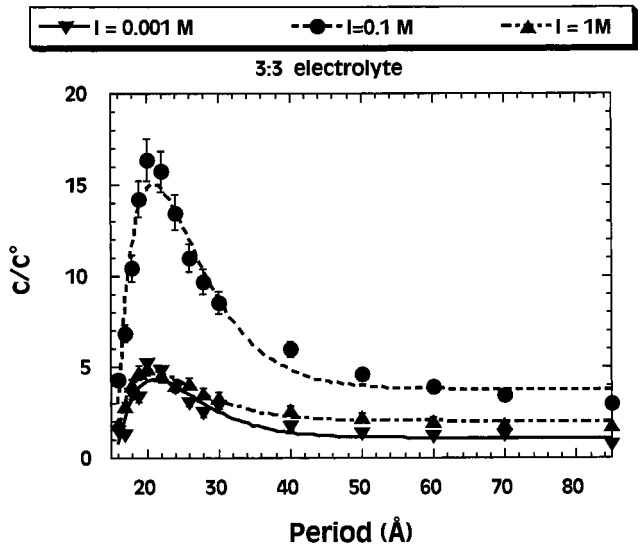

Figure 19. Accumulation of the 3:3 electrolyte within the charged interfaces.

The results obtained in the presence of a 3:3 electrolyte (Figures 17−19) are again very similar to those calculated for a 3:1 electrolyte, except for the decrease of the swelling pressure corresponding to $I = 1$ M (see Figures 12 and 17). The direct consequence of this pressure decrease is a damping of the repulsive barrier previously detected at $P = 25$ Å; in the presence large amounts of trivalent co-ion salts, the equation of state allows for the coexistence of two collapsed interfaces ($P = 16$ and 22 Å) (see Figure 17) instead of the coexistence of one collapsed phase ($P = 16$ Å) and one swollen phase ($P >$ 40 Å) (see Figure 12). Here also, the oscillation of the pressure coincides with a sudden enhancement of the overcharging ratio (Figure 18) and a large excess of the amount of confined salt (Figure 19). Finally, Figure 20 illustrates the different contributions to the longitudinal components of the swelling pressure calculated for charged lamellae in the presence of a 3:3 electrolyte at an ionic strength of 1 M. Entropic and contact contributions are of the same order of magnitude and cancel the electrostatic attraction at large separations. The contribution from the ion/ion contact force is maximized at $P = 20$ Å, as previously reported, because this period corresponds to an interlamellar separation equal to twice the ionic diam-

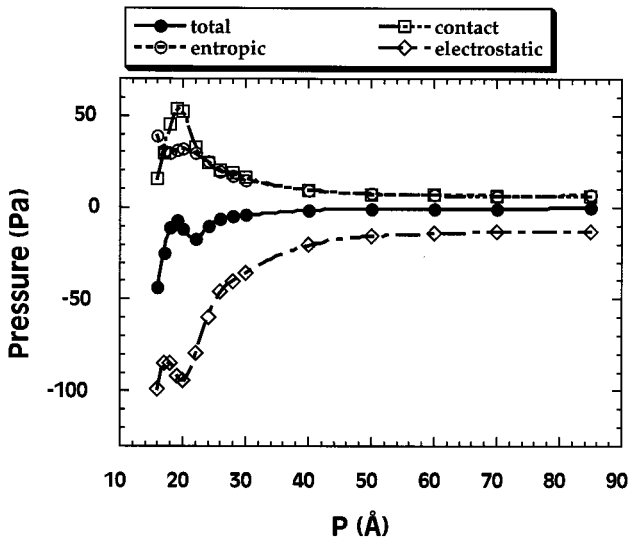

Figure 20. Total pressure (●) and its different contributions (entropic (○), contact (□), and electrostatic (◇), see text) calculated for charged interfaces in the presence of a 3:3 electrolyte ($I = 1$ M).

eter.[7,10] Note that more complex behavior is expected to occur if the ionic diameters of the cations and the anions are not exactly the same. Another conclusion resulting from this detailed analysis of the stability of the charged interfaces is the necessity of performing Monte Carlo simulations to extract quantitative predictions from the simple primitive model without introducing approximations or systematic errors.

D. Limitations and Prospects. This Monte Carlo study has established some links between the occurrence of the overcharging of infinite lamellae and the redispersion of coagulated interfaces, but this relationship is far from being a full equivalence. Overcharging is a general phenomenon that occurs even in the presence of monovalent counterions whereas coagulation and thus redispersion is not reported. Furthermore, it appears from these numerical simulations that the valence of the co-ions also plays an important role in the possible occurrence of redispersion. As a consequence, overcharging appears to be necessary but not sufficient for the redispersion of coagulated interfaces. Other indices of this interesting phenomenon include the accumulation of salt in the interlamellar domain and correlations between the layer of condensed counterions in contact with the charged interface and the nearest layer of co-ions. Finally, this study has also demonstrated that adding salt to charged interfaces does not screen out the electrostatic attraction resulting from the interionic correlations. In many cases, we detected some enhancement of the electrostatic attraction and even new cation/anion correlations that are responsible for the coexistence of swollen and collapsed phases.

All these results were obtained by using grand canonical Monte Carlo in the framework of the primitive model,[8] which neglects the atomic structure of the solvent molecules and the solid surfaces. In this approach, the solvent is replaced by a continuous medium characterized by its dielectric constant. This approximation becomes questionable not only at small interlamellar separations because of the strong layering[27] of the solvent by the solid surfaces but also at high salt concentrations because of the modification of the structure of the ion solvation sphere and the possible formation of contact ion pairs. The only possibility of going beyond this approximation is a molecular treatment[36−38] of these interfacial systems and salt solutions.

In this study, we have considered the simplest interfacial system (i.e., smooth lamellae with a regular squared network of surface charges). We have also neglected the possible lateral shift of the charged lamellae, which was recently shown to minimize the interfacial free energy.[39] Other distributions of surface sites may be considered, and Monte Carlo simulations must also be performed for other geometries (spheres, cylinders, etc.) to provide useful results for a larger class of colloidal materials including biological and synthetic polyions. As an example, similar conclusions have been reported from Monte Carlo simulations of the ionic concentration profiles within a cylindrical capillary.[40] For these reasons, this study must be considered to be a first approach that attempts to sketch the most important features of these complex systems.

IV. Conclusions

Grand canonical Monte Carlo simulation is a powerful tool in the investigation of the influence of salt addition on the stability of charged interfaces in equilibrium with a salt reservoir and may be used to describe, without any approximations, all of the electrostatic and excluded volume interactions incorporated into the primitive model. By contrast to previous qualitative predictions, adding salts of multivalent counterions to charged interfaces does not screen out the interionic correlations but rather enhances or even generates new counterion/co-ion correlations. These supplementary correlations are responsible for the coexistence between collapsed and swollen interfaces in connection with some inversion of the apparent charge of the interfaces and the accumulation of dissociated salt molecules within highly confined geometries. Unfortunately, no unique criteria emerge from our simulation data to characterize the experimental conditions sufficiently to induce the coexistence of collapsed and swollen phases and re-entrant behavior.

Acknowledgment. We cordially thank Drs. R. Setton, P. Levitz, and J.L. Raimbault for helpful discussions. The Monte Carlo simulations were performed either locally on workstations purchased with grants from Région Centre (France), on workstations of the Gage Laboratory (Palaiseau, France), or on the Nec supercomputer (IDRIS, France).

References and Notes

(1) Langmuir, I. *J. Chem. Phys.* **1938**, *6*, 873.
(2) Derjaguin, B.; Landau, L. D. *Acta Physicochim. URSS* **1941**, *14*, 635.
(3) Verwey, E. J. W.; Overbeek, J. T. G. *Theory of the Stability of Lyotropic Colloids*; Elsevier: New York, 1948.
(4) Kjellander, R.; Marcelja, S.; Pashley, R. M.; Quirk, J. P. *J. Chem. Phys.* **1990**, *92*, 4399.
(5) Greberg, H.; Kjellander, R.; Akesson, T. *Mol. Phys.* **1997**, *92*, 35.
(6) Delville, A.; Pellenq, R. J. M.; Caillol, J. M. *J. Chem. Phys.* **1997**, *106*, 7275.
(7) Pellenq, R. J. M.; Caillol, J. M.; Delville, A. *J. Phys. Chem. B* **1997**, *101*, 8584.
(8) Carley, D. D. *J. Chem. Phys.* **1967**, *46*, 3783.
(9) Delville, A.; Pellenq, R. J. M. *Mol. Simul.* **2000**, *24*, 1.
(10) Guldbrand, L.; Jönsson, B.; Wennerström, H.; Linse, P. *J. Chem. Phys.* **1984**, *80*, 2221.
(11) Valleau, J. P.; Ivkov, R.; Torrie, G. M. *J. Chem. Phys.* **1991**, *95*, 520.
(12) Linse P.; Lobaskin, V. *J. Chem. Phys.* **2000**, *112*, 3917.
(13) Allahyarov, E.; D'Amico, I.; Löwen, H. *Phys. Rev. Lett.* **1998**, *81*, 1334.
(14) Hribar, B.; Vlachy, V. *J. Phys. Chem. B* **2000**, *104*, 4218.
(15) Hakem, F.; Jokner, A.; Joany, J. F. *Macromolecules* **1998**, *31*, 8305.
(16) Netz, R. R.; Orland, H. *Europhys. Lett.* **1999**, *45*, 726.
(17) Dubois, M.; Zemb, Th.; Belloni, L.; Delville, A.; Levitz, P.; Setton, R. *J. Chem. Phys.* **1992**, *96*, 2278.

(18) Shklovskii, B. I. *Phys. Rev. Lett.* **1999**, *82*, 3268.
(19) Nguyen, T. T.; Rouzina, I.; Shklovskii, B. I. *J. Chem. Phys.* **2000**, *112*, 2562.
(20) Nguyen, T. T.; Grosberg, A. Y.; Shklovskii, B. I. *J. Chem. Phys.* **2000**, *113*, 1110.
(21) Nguyen, T. T.; Grosberg, A. Y.; Shklovskii, B. I. *Phys. Rev. Lett.* **2000**, *85*, 1568.
(22) Shklovskii, B. I. *Phys. Rev. E* **1999**, *60*, 5802.
(23) Perel, V. I.; Shklovskii, B. I. *Physica A* **1999**, *274*, 446.
(24) Adams, D. J. *Mol. Phys.* **1974**, *28*, 1241.
(25) Cooker, H. *J. Phys. Chem.* **1976**, *80*, 1084.
(26) Heerman, D. W. *Computer Simulation Methods in Theoretical Physics*; Springer-Verlag: Berlin, 1986.
(27) Israelachvili, J. C. *Intermolecular and Surface Forces*; Academic Press: London, 1985.
(28) Hansen, J. P.; McDonald, I. R. *Theory of Simple Liquids*; Academic Press: London, 1986.
(29) Heyes, D. M. *Phys. Rev. B: Condens. Matter* **1994**, *49*, 755.
(30) Viani, B. E.; Low, Ph. F.; Roth, C. B. *J. Colloid Interface Sci.* **1983**, *96*, 229.
(31) Legrand, P. *The Surface Properties of Silica*; Wiley & Sons: London, 1998.
(32) Allen, M. P.; Tildesley, D. J. *Computer Simulation of Liquids*; Clarendon Press: Oxford, 1994.
(33) Hummer, G. *Chem. Phys. Lett.* **1995**, *235*, 297.
(34) Kékicheff, P.; Marcelja, S.; Senden, T. J.; Shubin, V. E. *J. Chem. Phys.* **1993**, *99*, 6098.
(35) Vlachy, V. *Langmuir* **2001**, *17*, 399.
(36) Delville, A. *J. Phys. Chem.* **1993**, *97*, 9703.
(37) Chang, F. R. C.; Skipper, N. T.; Sposito, G. *Langmuir* **1998**, *14*, 1201.
(38) Teppen, B. J.; Rasmussen, K.; Bertsch, P. M.; Miller, D. M.; Schäfer, L. *J. Phys. Chem. B* **1997**, *101*, 1579.
(39) Meyer, S.; Delville, A. *Langmuir* **2001**, *17*, 7433.
(40) Hribar, B.; Vlachy, V.; Bhuiyan, L. B.; Outhwaite, C. W. *J. Phys. Chem. B* **2000**, *104*, 11522.